Nonresonant breakup effects in $^6\vec{Li}$+ ^{58}Ni elastic scattering at 70.5 MeV

K. Rusek
Soltan Institute for Nuclear Studies, Zaklad 1, Hoza 69, 00 681 Warsaw, Poland

N. M. Clarke, G. Tungate, and R. P. Ward*
School of Physics and Space Research, University of Birmingham, Edgbaston, Birmingham B15 2TT, United Kingdom
(Received 26 May 1995)

Recently published data for the elastic scattering of 70.5 MeV polarized ^{6}Li by ^{58}Ni have been compared with the results of coupled-channels calculations. The diagonal and off-diagonal potentials used in the analysis were generated from phenomenological α + ^{58}Ni and $\vec{d}$ + ^{58}Ni optical potentials via the cluster-folding method. Examined were the effects of projectile excitation to the three low-lying $T=0$ resonant states and to nonresonant continuum states in the energy range 0.63 MeV–10.03 MeV, relative to the $^6\text{Li}\rightarrow\alpha+d$ breakup threshold at 1.47 MeV. In common with earlier analyses, calculations limited to the resonant excited states reproduced the data only when the interaction and coupling potentials were renormalized. However, the inclusion of the nonresonant excited states removed the need for this renormalization. Calculations including both the resonant and nonresonant states yielded a description of the differential cross section data superior to that resulting from calculations limited to the resonant states even when the latter were performed with renormalized potentials. Calculations of the tensor analyzing powers reproduced the data well and favored a near zero value for the spectroscopic amplitude of the D-state admixture in the ^{6}Li ground state cluster wave function.

PACS number(s): 25.10.s, 24.10.Eq, 24.70.+s

I. INTRODUCTION

Thompson and Nagarajan [1] first demonstrated that the breakup of ^{6}Li into $\alpha+d$ plays a highly important role in the elastic scattering of ^{6}Li. Nishioka *et al.* then demonstrated that calculations of analyzing powers for polarized ^{6}Li scattering are highly sensitive to projectile excitation phenomena [2], making such analyses of polarization data a powerful probe of the structure of ^{6}Li. Since the study by Nishioka *et al.*, most analyses of polarized ^{6}Li scattering have focused on the effects of couplings between the ground and resonant excited states of ^{6}Li [3]. However, couplings to nonresonant excited states have recently been shown to be just as important [4,5].

Dee *et al.* [6] obtained data for the elastic scattering of polarized ^{6}Li by ^{58}Ni at 70.5 MeV and compared that data with the results of coupled-channels (CC) calculations performed using cluster-folding (CF) potentials. These calculations included couplings between the ground state of ^{6}Li and the three lowest-lying $\alpha+d$ resonances in ^{6}Li, at excitation energies of 0.72 MeV, 2.84 MeV, and 4.18 MeV above the $\alpha+d$ breakup threshold at 1.47 MeV, as well as couplings to the two lowest excited states of ^{58}Ni at 1.45 MeV and 2.45 MeV. Additionally, the second-rank tensor potential T_R, responsible for reorientation of the ^{6}Li ground state in the field of the target nucleus, was included in the calculations. In common with previous analyses, this study revealed that the data could not be reproduced without the introduction of two free parameters—renormalization factors N_r for the real and N_i for the imaginary parts of the diagonal and off-diagonal CF potentials. With $N_r=0.7, N_i=0.8$, the four angular distributions obtained in the experiment (differential cross section, first-rank tensor analyzing power iT_{11}, second-rank analyzing powers T_{20} and $^TT_{20}$) could be reproduced. It was found that the effect of the dynamic spin-orbit potential produced by channel coupling was much more important than the effect of the static CF spin-orbit potential. This confirmed the results of previous analyses of data obtained at energies between 15 and 60 MeV [4,5,7–13]. Another important finding of Dee *et al.* was that calculations of the second-rank tensor analyzing powers (TAP's) were sensitive to both the sign and the magnitude of b_D, the spectroscopic amplitude of the $L=2$ component of the ^{6}Li ground state cluster wave function.

The present work extends the study performed by Dee *et al.* by taking into account the effects of nonresonant continuum excited states of ^{6}Li. Only a few analyses of ^{6}Li scattering exist in which the effects of nonresonant continuum states have been investigated [4,5,8,14]. In none of them, however, was the second-rank tensor potential T_R included in the calculations. The main objective of the present study was to compare the effects of the nonresonant states on predictions of the second-rank TAP's with those due to ground state reorientation.

A CC analysis by Rusek *et al.* [5] of data for the elastic scattering of vector-polarized ^{6}Li by ^{26}Mg at 60 MeV, including both resonant and nonresonant excited states of the projectile, led to a good description of the differential cross section and first-rank TAP without any artificial renormalization of the CF potentials. This confirmed a prediction by Hirabayashi and Sakuragi [15] that, at bombarding energies greater than 10 MeV per nucleon, analyses of ^{6}Li scattering

*Present address: School of Sciences, Staffordshire University, College Road, Stoke-on-Trent ST4 2DE, United Kingdom.

TABLE I. Optical potentials. Potential depths are in MeV and geometric parameters are in fm. Woods-Saxon form factors were used for the real potentials and for the α + ^{58}Ni imaginary potential. A Woods-Saxon derivative form factor was used for the d + ^{58}Ni imaginary potential. The spin-orbit potential was of the Thomas form, while the tensor potential took the form proposed by Keaton and Armstrong [29].

System	V_0	r_0	a_0	W_s	W_d	r_i	a_i	$V_{s.o.}$	$r_{s.o.}$	$a_{s.o.}$	V_{T_R}	r_{T_R}	a_{T_R}	W_{T_R}	r_{IT_R}	a_{IT_R}	r_C	Ref.
α + ^{58}Ni	124.56	1.299	0.738	15.08	0	1.626	0.521										1.40	[18]
d + ^{58}Ni	76.7	1.32	0.51	0	10.8	0.98	1.27	7.11	1.12	0.23	1.62	0.95	0.34	1.11	1.11	0.85	1.30	[16]
^{6}Li = $d+\alpha$	90.0	1.20	0.65														1.30	[20]

would be free of renormalization. However, the data of Dee *et al.* [6] are a more stringent test of the continuum-discretized coupled-channels (CDCC) method, as they include second-rank TAP's, while the data of Ward *et al.* [13] were restricted to the first-rank TAP. Furthermore, the beam energy used by Dee *et al.* was chosen such that the d + ^{58}Ni optical model potential, required for the generation of the ^{6}Li + ^{58}Li CF potentials, could be adopted from the study of $\vec{d}$ + ^{58}Ni scattering at 22 MeV by Takei *et al.* [16]. In contrast, the earlier analysis by Rusek *et al.* [5] had to rely on a global parameterization for the d + ^{26}Mg potential. Thus an opportunity exists to perform a more reliable test of the prediction of Hirabayashi and Sakuragi [15].

II. CC CALCULATIONS

The CC calculations were performed using version FRX of the finite-range coupled-channels code FRESCO [17]. Couplings were included between the ground and excited states of ^{6}Li and between all excited states of ^{6}Li. Calculations with target excitation also included couplings between the excited states of the target. Couplings between the D-state component of the ^{6}Li ground state and excited states of ^{6}Li were not considered in the present analysis because b_D is so small. This approximation was adopted from the analysis by Nishioka *et al.* [2]. Reorientation couplings were also included for all states with nonzero spin.

A. Potentials

The diagonal and off-diagonal potentials employed were identical to those used by Dee *et al.*, [6] these being derived from empirical α + ^{58}Ni [18] and $\vec{d}$ + ^{58}Ni [16] optical model parameters by the CF method. The CF potentials yielded have been discussed in detail by Dee *et al.* [6]. The present analysis employed the CF potential set generated using set 2 of Takei *et al.* [16] for the d + ^{58}Ni channel. Takei *et al.* compared the results of TAP predictions for $\vec{d}$ + ^{90}Zr elastic scattering resulting from phenomenological tensor potentials with those derived from folded tensor potentials and found the two to be similar, although there was some overprediction of T_{21} in the case of the folded potential. Matsuoka *et al.* [19] did a similar comparison for the elastic scattering of polarized deuterons by ^{40}Ca and ^{208}Pb. While there were significant discrepancies between the predictions derived from phenomenological and folded potentials for the ^{208}Pb target, those for the ^{40}Ca target were almost identical. Thus it would seem that phenomenological and folded potentials for deuteron scattering are consistent for medium weight targets like ^{58}Ni, lending weight to the use of CF potentials to describe ^{6}Li scattering. The ^{6}Li$=\alpha+d$ cluster model potential was taken from Kubo *et al.* [20]. The input potential parameters are summarized in Table I.

B. Resonant projectile excitations

The $\alpha+d$ cluster model wave functions of the ^{6}Li ground state and the three $L=2$ resonances above the breakup threshold were adopted from the study by Dee *et al.* [6]. Excitation of the resonant states was incorporated using the *weak binding energy approximation*. The validity of this approximation was confirmed by Hirabayashi and Sakuragi [12] in their study of ^{6}Li + ^{26}Mg scattering at 44 MeV. The depth V_0 of the ^{6}Li$=\alpha+d$ cluster model potential was adjusted such that the binding energy of the state in question was reproduced.

C. Nonresonant projectile excitations

To account for nonresonant $\alpha+d$ breakup channels the ^{6}Li continuum was discretized into a set of momentum bins with respect to the momentum k of the $\alpha+d$ relative motion, as in the study by Rusek *et al.* [5]. The width of each momentum bin was set to 0.3 fm^{-1} for $L=0,1$ states and to 0.2 fm^{-1} for $L=2$, based on the results of detailed test calculations performed by Rusek *et al.* for ^{6}Li + ^{26}Mg scattering at 60 MeV [5]. In the CC calculations, each momentum bin was treated as an excited state of ^{6}Li at an excitation energy E_x equal to the mean energy of the bin and having spin I and parity $(-1)^L$, where L is the relative angular momentum between the α particle and the deuteron in the cluster system. The relative ^{6}Li + ^{58}Ni scattering wave functions were calculated at E_x and assumed to be energy independent within a particular bin. Following the findings of Hirabayashi, L was limited to the values 0,1, and 2 [4]. The model momentum space was limited to $0.2\leq k\leq 0.8$ fm^{-1}, again based on the results of Rusek *et al.* [5]. The details of the truncation and discretization of the ^{6}Li continuum are presented in Table II, where $E_{\max}$ and $E_{\min}$ represent the energy limits of the bins. The same information is presented diagrammatically in Fig. 1.

D. The D-state component of ^{6}Li$_{g.s.}$

There is recently an interest in the D-state component of the ground state wave functions of light nuclei [21], in particular for ^{6}Li [6,22,23]. According to the $\alpha+d$ cluster model of ^{6}Li [7] the spectroscopic amplitude b_D of the $L=2$ admixture to the ^{6}Li ground state wave function is related to the (very small) spectroscopic quadrupole moment of ^{6}Li. This amplitude is related within the model to the second-rank tensor potential T_R between ^{6}Li and a target nucleus. This provides a method for obtaining b_D from measurements of

TABLE II. Model space for ^{6}Li. The energies E_x, E_{min}, and E_{max} are measured relative to the $^6\text{Li}\rightarrow\alpha+d$ breakup threshold at 1.47 MeV. The energy E_x is the mean of E_{min} and E_{max}. The quantity σ is the predicted cross section for excitation of the state yielded by the seventeen-channel calculations.

L	I^π	E_x[MeV]	E_{min}[MeV]	E_{max}[MeV]	σ[mb]
0	1^+	−1.47			2441
0	1^+	2.27	0.63	3.92	16.3
0	1^+	6.98	3.92	10.03	2.1
1	0^-	2.27	0.63	3.92	2.05
1	0^-	6.98	3.92	10.03	0.75
1	1^-	2.27	0.63	3.92	6.2
1	1^-	6.98	3.92	10.03	2.0
1	2^-	2.27	0.63	3.92	10.6
1	2^-	6.98	3.92	10.03	3.2
2	3^+	0.72			14.8
2	3^+	4.08	2.51	5.65	2.3
2	3^+	7.84	5.65	10.03	3.7
2	2^+	2.84			8.3
2	2^+	7.84	5.65	10.03	2.1
2	1^+	4.18			4.1

the second-rank TAP's for ^{6}Li scattering. Since the T_R potential consists of two parts—one proportional to b_D and the other arising from the d + target second-rank tensor potential—precise knowledge of the latter from polarized deuteron scattering at the relevant energy is essential. Figure 2 depicts the components of the CF T_R tensor potential and illustrates the profound effects of varying the value of b_D.

E. Target excitation

The two lowest-lying excited states of ^{58}Ni (2^+ at 1.45 MeV and 4^+ at 2.45 MeV) were treated in the calculations as vibrational states. Quadrupole collective form factors were used. The Coulomb form factors were multiplied by the square root of the empirical value of the reduced transition probability $B(E2;\text{g.s.}\rightarrow 2^+)=695\ e^2\ \text{fm}^4$ [24], while the nuclear form factors were equal to the derivative of the CF central potentials multiplied by the deformation length $\delta=0.85$ fm [25]. The effects of mutual excitation of the target and projectile nuclei were not investigated in the present analysis, as Rusek *et al.* [11] reported this phenomenon to have little effect on predicted elastic scattering observables.

III. RESULTS

A. Differential cross section and first-rank TAP

The results of one-channel (optical model) calculations are shown as dot-dashed lines in Fig. 3. The differential cross section data were overpredicted for $\theta_{c.m.}>40°$ and underpredicted at more forward angles. The inclusion of couplings to the $L=2$ resonant states of ^{6}Li yielded the dashed lines in Fig. 3. The predicted backward angle differential cross section was reduced, the phase of the oscillations in the predicted cross section was shifted and a significant first-rank TAP was generated. The addition of nonresonant excitations to the coupling scheme, as listed in Table II, resulted in the dotted lines shown in Fig. 3. The differential cross section data are well described, although data for the first-rank TAP are overpredicted. The inclusion of excitation to the two excited states of ^{58}Ni affected the predicted differential cross section at the most backward angles and improved the overall description of the data, as shown by the solid curves in Fig. 3. The CF static spin-orbit potential was omitted in all the calculations depicted in Fig. 3, as its effect on the results was found to be negligible in comparison with the effects of channel-coupling [6].

Figure 4 compares the results of seventeen-channel calculations with the results of six-channel calculations performed using renormalized CF potentials. The angular distribution of the differential cross section data is better reproduced by the seventeen-channel calculation, involving couplings to the

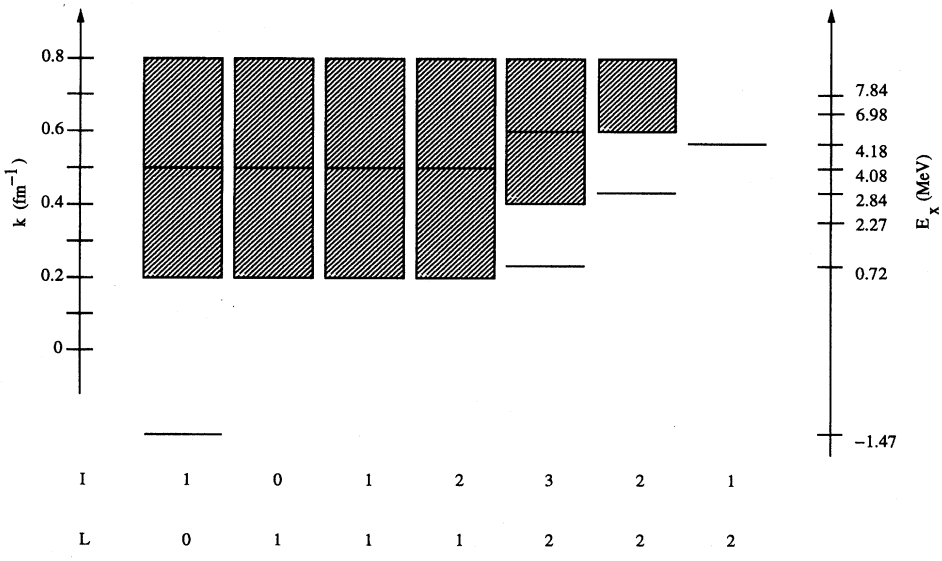

FIG. 1. Model space for ^{6}Li. The resonant excited states are depicted as lines, while the shaded areas represent the nonresonant excited states. The excitation energy E_x is measured relative to the $^6\text{Li}\rightarrow\alpha+d$ breakup threshold at 1.47 MeV.

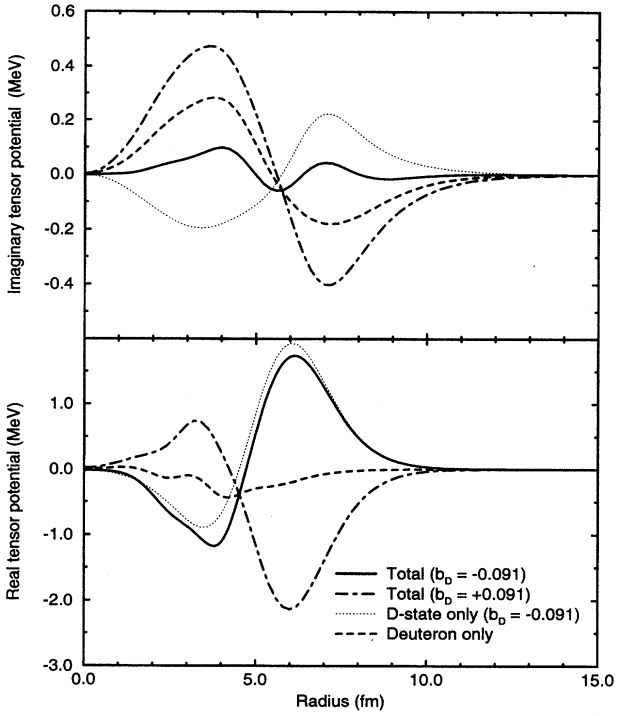

FIG. 2. Real and imaginary parts of the CF T_R tensor potential derived from the phenomenological potentials of Chang *et al.* [18] and Takei *et al.* [16].

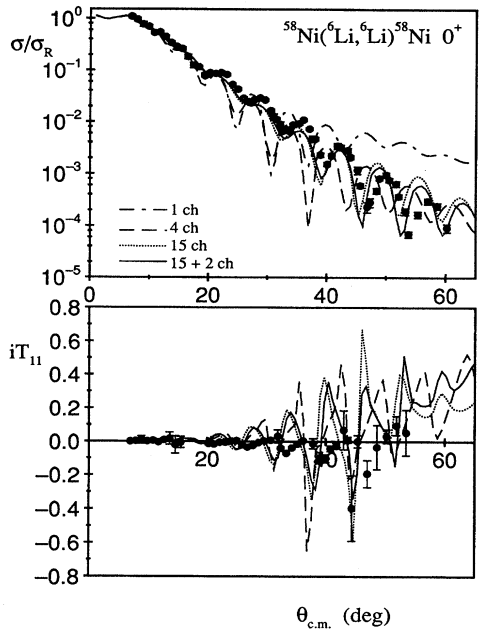

FIG. 3. Results of CC calculations for the differential cross section and first-rank TAP. The CF spin-orbit and T_R potentials were omitted in these calculations. The dot-dashed curves correspond to one-channel or optical model calculations, the dashed curves to four-channel calculations including the $L=2$ resonant states of ^{6}Li, the dotted curves to fifteen-channel calculations including the resonant and nonresonant excited states of ^{6}Li, and the solid curves to seventeen channel calculations including the resonant and nonresonant excited states of ^{6}Li and the first two excited states of ^{58}Ni.

resonant and nonresonant excited states of the projectile, than by calculations with couplings limited to the three resonant states of ^{6}Li using renormalized CF potentials. Unexpectedly, the description of the first-rank TAP is worse than that obtained by Dee *et al.* [6]. The calculated angular distribution of iT_{11} is out of phase with the experimental one, even at forward scattering angles where projectile couplings effects due to nonresonant states of ^{6}Li have a large impact on the differential cross section. The inclusion of the static CF spin-orbit potential did not alter this result.

B. Second-rank TAP's

The results of one-, four-, fifteen-, and seventeen-channel calculations of the second-rank TAP's are shown in Fig. 5. In these calculations, the T_R (ground state reorientation) potential was omitted in order that the effect of inelastic excitation would be more readily apparent. The meaning of the curves plotted in Fig. 5 is the same as for Fig. 3. Generally, projectile excitation produced a significant effect on the predicted second-rank TAP's. Excitation of the target affected the result at the most backward angles. The final description of the second-rank TAP data was very good, with only the minimum in the $^TT_{20}$ angular distribution around $\theta_{c.m.}\approx 45°$ not satisfactorily reproduced by the calculations.

The calculations were found to be sensitive to the sign and value of the D-state spectroscopic amplitude b_D, as reported by Dee *et al.* [6]. When a second-rank T_R tensor potential corresponding to $b_D=-0.091$, the value calculated from a small negative quadrupole moment of ^{6}Li, was used in the calculations it affected the predicted angular distributions of T_{20} and $^TT_{20}$ most dramatically at the most backward angles, as shown by the dotted lines in Figure 6. Comparison of the predictions in Fig. 6 with those in Fig. 5 indicates that the description of the T_{20} data was best when the tensor potential was omitted. Changing the sign of b_D resulted in a much worse description of the $^TT_{20}$ data (dashed curves in Fig. 6). The results of calculations with

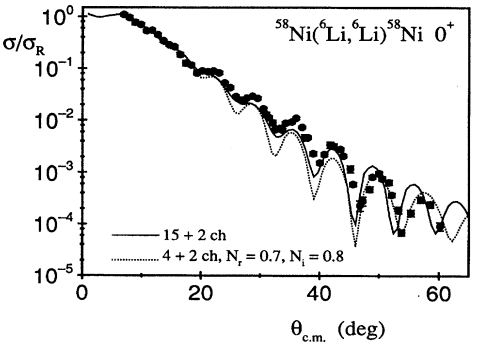

FIG. 4. Comparison of CC calculations performed using the full model space (seventeen channels, solid curve) with calculations performed using a model space limited to the four resonant states of ^{6}Li plus the two excited states of ^{58}Ni and CF potentials renormalized with $N_r=0.7, N_i=0.8$ (six channels, dotted curve).

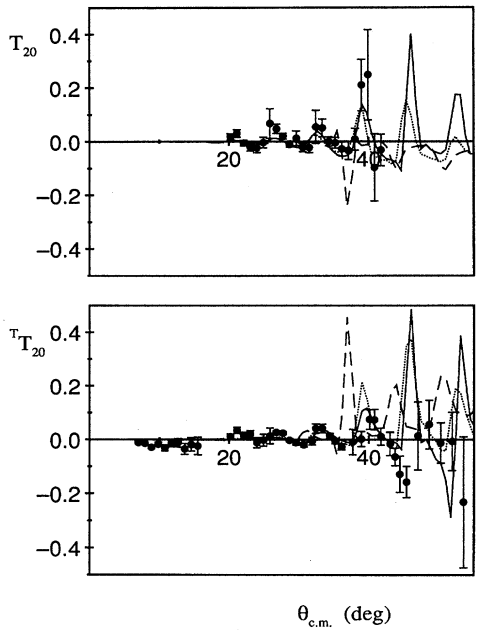

FIG. 5. CC predictions for the second-rank TAP's. The meanings of the curves are the same as in Fig. 3.

$b_D = -0.045$, i.e., half the value derived from the quadrupole moment, described the data better, as shown by the solid curves in Fig. 6. Nevertheless this description was worse than that obtained without the tensor potential (solid curves in Fig. 5). The results of calculations of T_{20} and ${}^{T}T_{20}$ with $b_D = 0$ were very similar to those with the T_R potential omitted. These observations suggest that the sign of the spectroscopic amplitude should be negative but that its value should be very close to zero. Calculations of the first-rank TAP were found to be only weakly sensitive to the value of b_D.

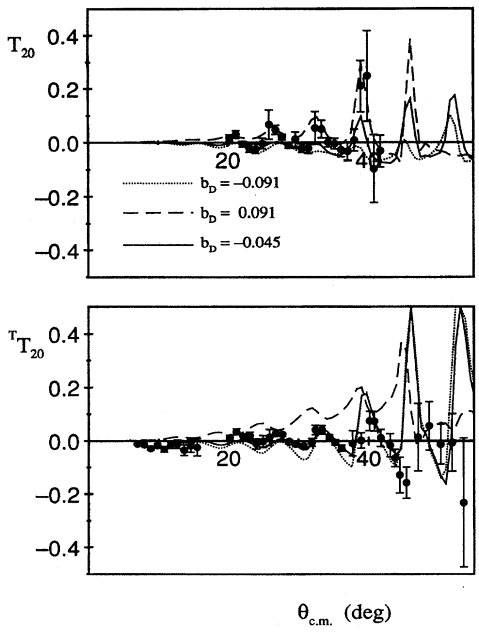

FIG. 6. Results of seventeen-channel calculations showing the dependence of the predicted second-rank TAP's T_{20} and ${}^{T}T_{20}$ on the spectroscopic amplitude b_D of the D-state component of the ^{6}Li ground state wave function.

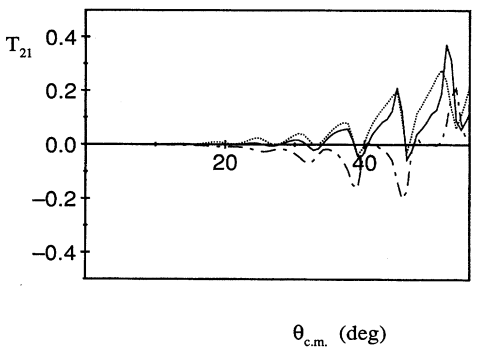

FIG. 7. Results of seventeen-channel calculations for the TAP T_{21}. The solid line corresponds to a calculation with the T_R potential omitted, the dotted line to a calculation with $b_D = -0.091$, and the dot-dashed line to a calculation with $b_D = 0.091$.

The analyses by Reber *et al.* [26,27] of polarized ^{6}Li scattering by ^{12}C at 30 MeV found that reorientation of the ground state of ^{6}Li was a major contribution to the elastic scattering TAP T_{21}. A similar conclusion has also been reported by Kerr *et al.* [28]. The present calculations did not confirm these findings. Here, all second-rank TAP's exhibited similar sensitivity to the T_R potential. Figure 7 shows the results of calculations of T_{21} without the T_R potential (solid curve) and with two different T_R potentials corresponding to $b_D = \pm 0.091$. The results with $b_D = -0.091$ and without the T_R potential are quite similar, while the results with $b_D = +0.091$ are different even at forward angles. The results of calculations of T_{21} with $b_D = 0$ were similar to those with the T_R potential omitted, as was observed for calculations of T_{20} and ${}^{T}T_{20}$.

IV. SUMMARY

The present analysis of polarized ^{6}Li scattering by ^{58}Ni at 70.5 MeV confirmed the results of Rusek *et al.* for ^{6}Li + ^{26}Mg scattering at 60 MeV [5]. CC calculations with CF potentials, including a nonresonant $\alpha + d$ breakup continuum discretized in the manner described by Rusek *et al.*, yielded a good description of the elastic scattering differential cross section without any renormalization of the interaction and coupling potentials. The description of the differential cross section data, especially at forward angles, was better than that yielded by CC calculations which included only the resonant excited states of ^{6}Li and used renormalized CF potentials.

The present analysis did not lead to a good description of the first-rank TAP. The calculated values of iT_{11} originated from a dynamic spin-orbit potential generated by channel coupling, as found in many previous studies at lower energies; the effect of the static CF spin-orbit potential was very small. The angular distribution of iT_{11} emerging from the calculations was out of phase with the measured one. The reason for this discrepancy was not found.

Couplings to the $\alpha + d$ resonant and nonresonant states of

^{6}Li were found to be mainly responsible for the second-rank TAP's. Angular distributions of T_{20} and $^TT_{20}$ were well reproduced by the calculations. The effect of the tensor potential responsible for the reorientation of ^{6}Li ground state was important but nothing conclusive could be said about the spectroscopic amplitude of the D-state component of the ^{6}Li ground state wave function. The best description of the experimental data was obtained without the tensor potential, which could be interpreted within the $^6\text{Li}=\alpha+d$ cluster model as an indication that this amplitude should be near zero.

ACKNOWLEDGMENTS

N.M.C., G.T., and R.P.W. acknowledge the support of the Engineering and Physical Sciences Research Council of the United Kingdom.

[1] I.J. Thompson and M.A. Nagarajan, Phys. Lett. **106B**, 163 (1981).
[2] H. Nishioka, R.C. Johnson, J.A. Tostevin, and K.-I. Kubo, Phys. Rev. Lett. **48**, 1795 (1982).
[3] D. Fick, G. Grawert, and Irena M. Turkiewicz, Phys. Rep. **214**, 1 (1992).
[4] Y. Hirabayashi, Phys. Rev. C **44**, 1581 (1991).
[5] K. Rusek, N.M. Clarke, and R.P. Ward, Phys. Rev. C **50**, 2010 (1994).
[6] P.R. Dee, C.O. Blyth, H.D. Choi, N.M. Clarke, S.J. Hall, O. Karban, I. Martel-Bravo, S. Roman, G. Tungate, R.P. Ward, N.J. Davis, D.B. Steski, K.A. Connell, and K. Rusek, Phys. Rev. C **51**, 1356 (1995).
[7] H. Nishioka, J.A. Tostevin, R.C. Johnson, and K.-I. Kubo, Nucl. Phys. **A415**, 230 (1984).
[8] H. Ohnishi, M. Tanifuji, M. Kamimura, Y. Sakuragi, and M. Yahiro, Nucl. Phys. **A415**, 271 (1984).
[9] G. Windham, H. Nishioka, J.A. Tostevin, and R.C. Johnson, Phys. Lett. **138B**, 253 (1984).
[10] Y. Sakuragi, M. Kamimura, M. Yahiro, and M. Tanifuji, Phys. Lett. **153B**, 372 (1985).
[11] K. Rusek, J. Giroux, H.J. Jänsch, H. Vogt, K. Becker, K. Blatt, A. Gerlach, W. Korsch, H. Leucker, W. Luck, H. Reich, H.-G. Völk, and D. Fick, Nucl. Phys. **A503**, 223 (1989).
[12] Y. Hirabayashi and Y. Sakuragi, Nucl. Phys. **A536**, 375 (1992).
[13] R.P. Ward, N.M. Clarke, K.I. Pearce, C.N. Pinder, C.O. Blyth, H.D. Choi, P.R. Dee, S. Roman, G. Tungate, and N.J. Davis, Phys. Rev. C **50**, 918 (1994).
[14] M. Kamimura, Y. Sakuragi, M. Yahiro, and M. Tanifuji, in *Proceedings of the Sixth International Symposium on Polarization Phenomena in Nuclear Physics,* Osaka, 1985, edited by M. Kondo, S. Koyabashi, M. Tanifuji, T. Yamazaki, K.-I. Kubo, and N. Onishi (Physical Society of Japan, Tokyo, 1986), p. 205.
[15] Y. Hirabayashi and Y. Sakuragi, Phys. Lett. B **258**, 11 (1991).
[16] M. Takei, Y. Aoki, Y. Tagishi, and K. Yagi, Nucl. Phys. **A472**, 41 (1987).
[17] I.J. Thompson, Comput. Phys. Rep. **7**, 167 (1988).
[18] H.H. Chang, B.W. Ridley, T.H. Braid, T.W. Conlon, E.F. Gibson, and N.S.P. King, Nucl. Phys. **A270**, 413 (1976).
[19] N. Matsuoka, H. Sakai, T. Saito, K. Hosono, M. Kondo, H. Ito, K. Hatanaka, T. Ichihara, A. Okihana, K. Imai, and K. Nisimura, Nucl. Phys. **A455**, 413 (1986).
[20] K.-I. Kubo and M. Hirata, Nucl. Phys. **A187**, 186 (1972).
[21] A.M. Eiro and F.D. Santos, J. Phys. G **16**, 1139 (1990).
[22] J.E. Bowsher, T.B. Clegg, H.J. Karwowski, E.J. Ludwig, W.J. Thompson, and J.A. Tostevin, Phys. Rev. C **45**, 2824 (1992).
[23] V. Punjabi, C.F. Perdrisat, E. Cheung, J. Yonnet, M. Boivin, E. Tomasi-Gustafsson, R. Siebert, R. Frascaria, E. Warde, S. Belostotsky, O. Miklucho, V. Sulimov, R. Abegg, and D.R. Lehman, Phys. Rev. C **46**, 984 (1992).
[24] S. Raman, C.H. Malarkey, W.T. Milner, C.W. Nestor, Jr., and P.H. Stelson, At. Data Nucl. Data Tables **36**, 1 (1987).
[25] A. Nadasen, M. McMaster, M. Fingal, J. Tavormina, J.S. Winfield, R.M. Ronningen, P. Schwandt, F.D. Becchetti, J.W. Jänecke, and R.E. Warner, Phys. Rev. C **40**, 1237 (1989).
[26] E.L. Reber, K.W. Kemper, P.V. Green, P.L. Kerr, A.J. Mendez, E.G. Myers, and B.G. Schmidt, Phys. Rev. C **49**, R1 (1994).
[27] E.L. Reber, K.W. Kemper, P.V. Green, P.L. Kerr, A.J. Mendez, E.G. Myers, B.G. Schmidt, and V. Hnizdo, Phys. Rev. C **50**, 2917 (1994).
[28] P.L. Kerr, K.W. Kemper, P.V. Green, K. Mohajeri, E.G. Myers, D. Robson, and B.G. Schmidt, Phys. Rev. C (to be published).
[29] P.W. Keaton, Jr. and D.D. Armstrong, Phys. Rev. C **8**, 1692 (1973).